Petroleum Science 23 (2026) 4280–4295

Contents lists available at ScienceDirect

Petroleum Science

journal homepage: www.keaipublishing.com/en/journals/petroleum-science

Original Paper

Energy-driven damage constitutive model of thermal insulation materials for deep rock in-situ temperature-preserved coring

Zi-Jie Wei [a,b], Zhi-Qiang He [a,b,*], Ling Chen [b,c], Bo Yu [b,c], Jian-Ping Yang [b,d], Hai-Shu Bai [b,c], He-Ping Xie [a,b,e]

[a] State Key Laboratory of Hydraulics and Mountain River Engineering, College of Water Resource and Hydropower, Sichuan University, Chengdu, 610065, Sichuan, China
[b] State Key Laboratory of Intelligent Construction and Healthy Operation and Maintenance of Deep Underground Engineering, Sichuan University, Chengdu, 610065, Sichuan, China
[c] College of Mechanical Engineering, Sichuan University, Chengdu, 610065, Sichuan, China
[d] College of Polymer Science and Engineering, Sichuan University, Chengdu, 610065, Sichuan, China
[e] Guangdong Provincial Key Laboratory of Deep Earth Sciences and Geothermal Energy Exploitation and Utilization, Institute of Deep Earth Sciences and Green Energy, College of Civil and Transportation Engineering, Shenzhen University, Shenzhen, 518060, Guangdong, China

a r t i c l e i n f o

Article history:
Received 26 June 2025
Received in revised form
4 February 2026
Accepted 13 April 2026
Available online 21 April 2026

Edited by Xi Zhang

Keywords:
In-situ temperature-preserved coring (ITP-Coring)
High-temperature and high-pressure (HTHP) environments
Hollow glass microsphere/epoxy thermal insulation materials (HGM/EP materials)
Energy evolution behaviour
Statistical damage constitutive model

a b s t r a c t

Accurate evaluation of deep oil and gas reservoirs critically depends on key properties such as rock porosity and permeability, which are significantly affected by high-temperature conditions in deep formations. In-situ temperature-preserved coring (ITP-Coring) is a prerequisite for reliable assessment of deep rock properties, with thermal insulation materials serving as its key component. This study investigates the performance variation law and damage evolution characteristics of thermal insulation materials under high-temperature and high-pressure conditions. The findings show that at elevated temperatures, the material compressive strength decreases to one-fourth to one-fifth of its value at room temperature, while the peak compressive strain increases by two to three times. Furthermore, the energy evolution and damage characteristics of the hollow glass microsphere/epoxy thermal insulation materials (HGM/EP materials) during uniaxial compression were analyzed, and an energy-driven statistical damage constitutive model was established, which effectively predicts the stress–strain behaviour of HGM/EP materials after temperature-pressure preconditioning. The correlation between initial damage d and pretreatment temperature and pressure was also examined. It was found that when the pretreatment pressure is below 100 MPa, the threshold temperature at which initial damage sharply increases is 100 °C. An initial damage evolution model considering temperature and pressure effects was established, and the relationship between damage rate, temperature, pressure and initial damage was analyzed. The research results provide a theoretical basis for the application of thermal insulation materials under extreme conditions in deep ITP-Coring operations.
© 2026 The Authors. Publishing services by Elsevier B.V. on behalf of KeAi Communications Co. Ltd. This is an open access article under the CC BY-NC-ND license (http://creativecommons.org/licenses/by-nc-nd/4.0/).

t t

As the Earth's resources continue to be exploited, the gradual depletion of shallow subsurface deposits has driven resource exploration and development toward greater depths (Xie et al., 2015, 2019, 2023). In the context of plentiful oil and gas resources, China has initiated two ultra-deep scientific exploration wells: the Deep Earth TK1 Well and the Deep Earth CK1 Well. Notably, the TK1 Well surpassed the 10,000 m mark on March 4, 2024, achieving a final drilled depth of 10,910 m. Concurrently, the CK1 Well is currently being drilled toward its target depth of 10,520 m (Sun et al., 2024). Deep oil and gas resources are in high-temperature environments, with a geothermal gradient of up 30–50 °C/km (Liu et al., 2016). High temperatures can markedly affect key properties such as rock permeability and porosity, which are critical for accurate assessment of deep subsurface oil and gas reserves (Chandra et al., 2021; Lin et al., 2023; Saif et al., 2017). Therefore, accurate evaluation of reservoir rock characteristics is a

* Corresponding author.
E-mail address: hzqscu@scu.edu.cn (Z.-Q. He).
Peer review under the responsibility of China University of Petroleum (Beijing).

https://doi.org/10.1016/j.petsci.2026.04.018
1995-8226/© 2026 The Authors. Publishing services by Elsevier B.V. on behalf of KeAi Communications Co. Ltd. This is an open access article under the CC BY-NC-ND license (http://creativecommons.org/licenses/by-nc-nd/4.0/).

6 0 9

6 : 4 6 6

: -

4 4

; < 2

1% : ')') 3: : 2 1 : ')'+

2 102 ')'+ D : ')'/ ')'+ 3

! 3 ; 785

1% : ')' . ')'/ 3: 6 2

- 02 ! : "

: 4 : "

1 2 3 9 4

6 : 9

! 4

6 6 : 2

4

02 : -

1 : ')') ')" D# : ')" 3: 4 <

4 5 6

1 785 3 6 2 : 2

4 785

1 : ')'+ 3: 2 : ,

6 4

02 ! : 2

785

2 : 02 ! :

& 6

6 6

1 : ')' . D! : ')'/ D" : ')') 3:

8 4 4

1

') . * D! : ')' . D# : ')" D$: ')" 3

1 : ') . (D 9 7 '))C D@

') . CD2 : ')' . D- : ')" 3

17 : ') . I D$: ') . I D :

')'* D : ')'+ 3: 2 4

<

: ,

$: 1')'+3 4

9 5

9 : : 1') . /3 <

6 : : 1')"3

'* !

. *) !: ! 1')'/3

< 4

4

: - 1') . C3

: 1')')3 6 78

() 8

4

: : 1')"3

4

: : 1')" ')'/3

: : 1')'*3

6

4 6 9 4

9 2

:

1212 (

"

>+(78 1/ 8

$ G $ 3 9 4

+)J *)J: 2 6 * .

6 1? % $ 8 ! 3

< ' + < 18

" ! 3: 2

. ' ') : 2 9

785

1 : ')'* 3:

1212 , ' ((

0 4 785 4 4

@ 0 $ $ 1$ >

0 ! 8 @ G

$ G 3 <

6 . () !

')) 8 9 : 2

/ !

' 8 4 . :* . :I !5

: 4

4 4 4

1$: ')'* 3: , 4

A 1'* *) .)) . *) !3 1) *) .))

. +) 8 3: 2 . (

: $ 9

1 : ')'* 3:

"

>+(78

785 4 : , 6 >+(

+) . +) 2. *) 785 4 +)J

K46 microsphere volume fraction that was treated at 140 MPa and 150 °C.

2.3. Testing method for physical and mechanical properties

The mass of the HGM/EP materials before and after temperature-pressure pretreatment is measured as m_1 and m_2, respectively. The mass change is calculated using the following Eq. (1):

$$=\frac{m_2 - m_1}{m_1} \times 100\% \quad (1)$$

Quantification of heat transfer characteristics in the HGM/EP materials was performed via the TPS2500S hot disk system. Mechanical properties evaluation employed an Instron electromechanical testing platform configured for uniaxial compression characterization. During both the thermal conductivity and mechanical property tests, the materials were maintained at their corresponding pretreatment temperatures for measurement. Detailed testing procedures were described in previous studies (Wei et al., 2025).

3 t t t t

3.1. Analysis of physical properties

Fig. 1 delineates the interdependent variations in water absorption rate and heat transfer coefficients after different temperature-pressure pretreatment. The trends in the changes in thermal conductivity are highly consistent with those of the water absorption rate. When the pressure is up to 50 MPa, the water absorption rate of the material increases with the rising pretreatment temperature, and the rate of increase becomes more significant. Correspondingly, the thermal conductivity of the material also increases. At pressures not exceeding 100 MPa, the temperature threshold of a remarkable rise in water absorption rate is approximately 100 °C. However, when the pressure reaches 140 MPa, the temperature threshold of a noticeable rise in water absorption drops to 50 °C, with the threshold for the K46-f50 material being even lower.

It can be observed that pressure is the dominant factor in material water absorption. Under high hydrostatic pressure, fluid penetration is facilitated, damaging the interface between the microspheres and the substrate. This damage results in the cracking of the microsphere. The infiltrated water, an efficient thermal conductor, significantly increases the thermal conductivity of the material. Elevated temperature also plays a key role by increasing the molecular chain mobility, thereby further promoting heat transfer.

3.2. Analysis of mechanical properties

As shown in Fig. 2, the variations in elastic modulus E, compressive strength $_c$, and the corresponding compressive strain at the peak point (hereafter referred to as peak point compressive strain ε_c) are presented as functions of pretreatment temperature under different hydrostatic pressures. With increasing temperature, the compressive strength $_c$ and elastic modulus E decrease consistently. Furthermore, the extent of reduction in compressive strength with temperature exhibits a clear dependence on the pretreatment pressure.

At a pretreatment pressure is 0 MPa, the rate of decrease in compressive strength with temperature follows a two-stage pattern: slow initially, then fast. When the pretreatment pressure is increased but does not exceed 100 MPa, the decrease in compressive strength with temperature exhibits an approximately linear trend. The rate of decrease is similar to the average rate of the two-stage decline observed under atmospheric pressure. While the hydrostatic pressure rises to 140 MPa, the rate of decrease again shows a two-stage pattern, but with the sequence reversed: fast initially, then slow. The transition temperature for this rate change is consistent with that under atmospheric pressure treatment, occurring at approximately 100 °C. In summary, compressive strength decreases with increasing temperature at all pretreatment pressures, and higher pressure accelerates this reduction.

The peak point compressive strain ε_c exhibits a distinct temperature threshold. Below this threshold, εc remains nearly constant, whereas it increases rapidly once the temperature is exceeded. At pressures $\leq$100 MPa, this threshold is approximately 100 °C. When the pressure reaches 140 MPa, the threshold drops to 50 °C or lower. Furthermore, the higher the pressure, the increase in compressive strain at the peak point. This behavior is consistent with the trend observed for water absorption, indicating that water infiltrated under high pressure facilitates plastic deformation. Concurrently, elevated temperature enhances the molecular chain mobility of the HGM/EP composite, promoting a transition

Variation curves of physical properties of HGM/EP materials.

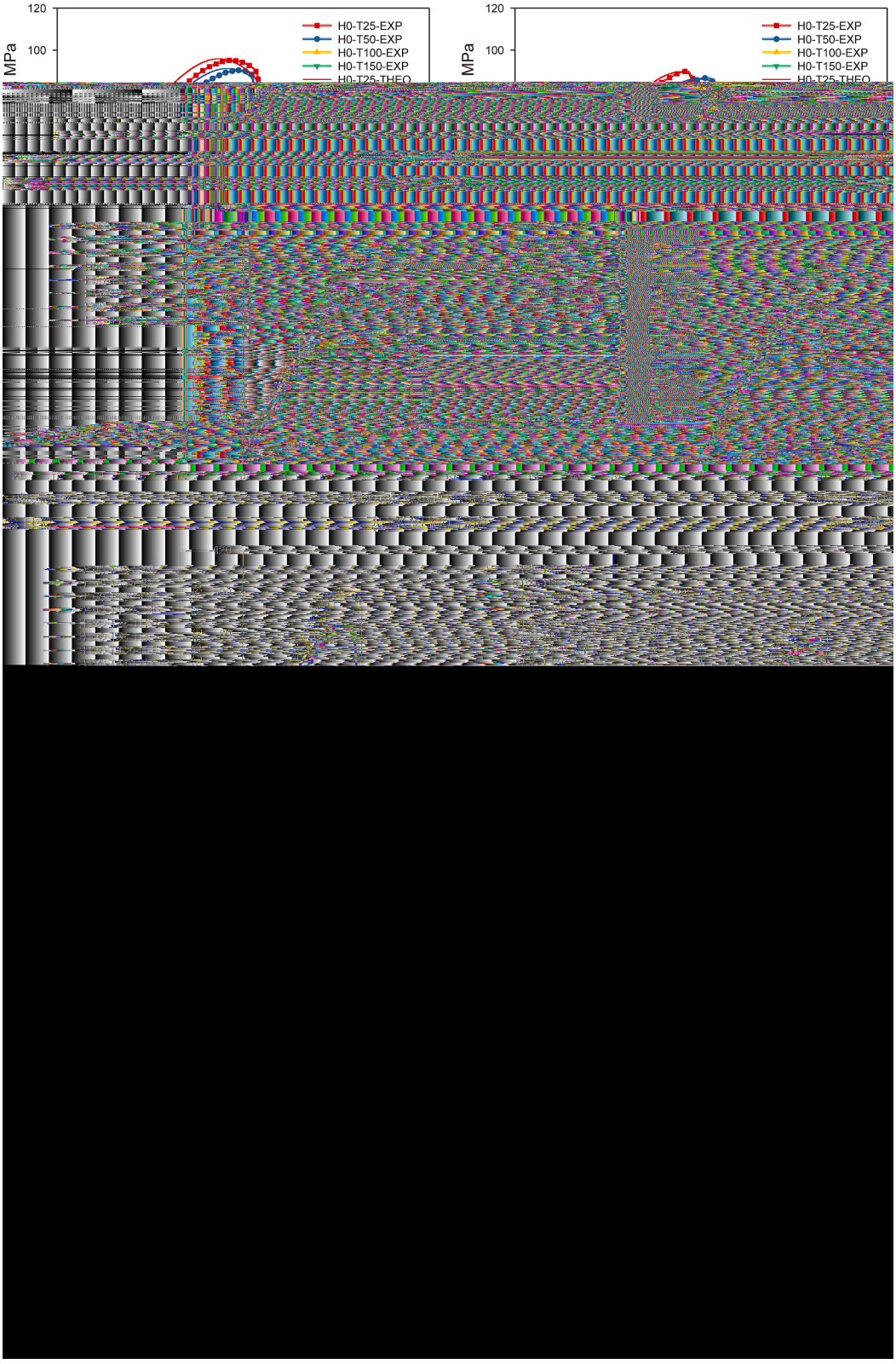

8 Predicted values from the statistical damage constitutive model and experimental stress–strain curves of HGM/EP materials at different temperature and pressure situations.

order to reduce the damage accumulation rate of insulation materials under HTHP conditions, it is recommended to minimize and . This can be achieved in future insulation material optimization by enhancing microsphere strength, improving interfacial bonding, and increasing the thermal resistance of the matrix.

5 C t t t t t t t t – t

To further analyze

effect. This shielding effect ultimately reduces the damage rate of the HGM/EP materials under uniaxial compression.

6 C

Regarding the performance changes of HGM/EP materials after temperature-pressure pretreatment, the variation laws of their physical and mechanical properties were analyzed. The energy evolution behavior during the uniaxial compression was explored, and a statistical damage constitutive model was established. The correlation between initial damage and damage rate with temperature and pressure were discussed. The main conclusions are as follows:

1. The variation rules of the properties of K46-f40 and K46-f50 HGM/EP materials after HTHP pretreatment were analyzed. High pressure is the primary factor leading to increased water absorption in the material. The infiltration of high-pressure water causes microsphere fracture, and the subsequent filling of the cavities establishes interconnected pathways for heat transfer, thereby enhancing thermal conductivity. Simultaneously, elevated temperature accelerates water infiltration and increases molecular chain mobility, further contributing to the rise in thermal conductivity. Furthermore, increasing pretreatment temperature softens the epoxy matrix, causing a transition from brittle to plastic failure and resulting in three characteristic types of stress-strain curves. High pressure facilitates this brittle-to-ductile transition.
2. Based on energy analysis, the damage evolution of HGM/EP materials during uniaxial compression after different temperature-pressure pretreatments was elucidated. When the pretreatment pressure does not exceed 50 MPa, the energy evolution is characterized by a transition at 100 °C from a regime dominated by elastic strain energy storage in the matrix to one governed by energy dissipation through matrix plastic deformation and microsphere damage. At elevated temperatures approaching the glass transition temperature, the epoxy matrix undergoes a progressive transition, leading to a deformation mechanism dominated by plastic flow. This is characterized by a continuous increase in energy dissipation.
3. A statistical damage constitutive model was developed for the HGM/EP composite. The model employs the dissipated energy weight factor ( ) and the stiffness degradation factor ( ) to assess the effects of temperature-pressure pretreatment on mechanical properties. The introduced weighting coefficients (,) reveal that, as α increases, the variation in the damage evolution rate (d*D*/d) with respect to a characteristic element strength follows one of two patterns: an initial increase followed by a decrease, or an initial decrease followed by an increase. The constructed model provides accurate predictions of the stress–strain response. The constructed initial damage evolution model indicates that the pre-treatment temperature is the key factor governing the accumulation of initial damage *d*, while the temperature-pressure coupling further exacerbates damage. Based on the integrated analysis of the physical-mechanical properties and damage evolution of both K46-f40 and K46-f50 thermal insulation materials, they are considered suitable for in-situ deep rock coring applications at temperatures up to 100 °C and pressures up to 100 MPa.

C t t t t t t

- : Writing – review & editing, Writing – original draft, Investigation, Data curation. - : Writing – review & editing, Visualization, Supervision, Investigation, Funding acquisition, Data curation. C : Investigation, Formal analysis, Data curation. : Investigation, Formal analysis, Data curation. - : Investigation, Formal analysis, Data curation. - : Investigation, Formal analysis, Data curation. - : Supervision, Resources, Project administration, Methodology, Conceptualization.

t t t t

The authors declare that they have no known competing financial interests or personal relationships that could have appeared to influence the work reported in this paper.

t

This work was supported by the National Natural Science Foundation of China (Grant No. 52304033), China Postdoctoral Science Foundation (Grant No. 2025T180116), Coal-Major Project (Grant No. 2025ZD1700902) and Ministry of Education of China (Grant No. JYB2025XDXM311).

Abedin, R., Feng, X., Pojman Jr., J., et al., 2022. A thermoset shape memory polymer-based syntactic foam with flame retardancy and 3D printability. ACS Appl. Polym. Mater. 4 (2), 1183–1195. https://doi.org/10.1021/acsapm.1c01596.
Bao, F., Wang, J., Wang, J., et al., 2020. Static and impact responses of syntactic foam composites reinforced by multi-walled carbon nanotubes. J. Mater. Res. Technol-JMRT 9 (6), 12391–12403. https://doi.org/10.1016/j.jmrt.2020.08.079.
Cao, S., Ma, N., Zhang, Y., et al., 2023. Fabrication, mechanical properties, and multifunctionalities of particle reinforced foams: A review. Thin-Walled Struct. 186, 110678. https://doi.org/10.1016/j.tws.2023.110678.
Chandra, D., Bakshi, T., Vishal, V., 2021. Thermal effect on pore characteristics of shale under inert and oxic environments: Insights on pore evolution. Microporous Mesoporous Mater. 316, 110969. https://doi.org/10.1016/j.micromeso.2021.110969.
Chen, Y., Wang, J., Wen, S., et al., 2021. Zinc phosphate coated modified hollow glass beads and their thermal insulation and anticorrosion performance in coatings. Ceram. Int. 47 (16), 23507–23517. https://doi.org/10.1016/j.ceramint.2021.05.067.
Deng, J.A., Cu, D.S., 2011. On a statistical damage constitutive model for rock materials. Comput. Geosci. 37 (2), 122–128. https://doi.org/10.1016/j.cageo.2010.05.018.
Doddamani, M., 2019. Effect of surface treatment on quasi-static compression and dynamic mechanical analysis of syntactic foams. Compos Pt B-Eng. 165, 365–378. https://doi.org/10.1016/j.compositesb.2019.01.076.
Garcia, C.D., Shahapurkar, K., Doddamani, M., et al., 2018. Effect of arctic environment on flexural behavior of fly ash cenosphere reinforced epoxy syntactic foams. Compos Pt B-Eng. 151, 265–273. https://doi.org/10.1016/j.compositesb.2018.06.035.
He, Z., Xie, H., Gao, M., et al., 2024a. In situ temperature-preserved coring for deep oil and gas reservoir: thermal insulation materials. J. Rock Mech. Geotech. Eng. 17 (9), 5601–5614. https://doi.org/10.1016/j.jrmge.2024.10.008.
He, Z.Q., Xie, H.P., Chen, L., et al., 2024b. Research on thermal insulation materials properties under HTHP conditions for deep oil and gas reservoir rock ITP-Coring. Pet. Sci. 21 (4), 2625–2637. https://doi.org/10.1016/j.petsci.2024.03.005.
He, Z.Q., Xie, H.P., Gao, M.Z., et al., 2020. Design and verification of a deep rock corer with retaining the in situ temperature. Adv. Civ. Eng. 2020 (1), 8894286. https://doi.org/10.1155/2020/8894286.
He, Z.Q., Yang, Y., Yu, B., et al., 2022. Research on properties of hollow glass microspheres/epoxy resin composites applied in deep rock in-situ temperature-preserved coring. Pet. Sci. 19 (2), 720–730. https://doi.org/10.1016/j.petsci.2021.10.028.
Huang, R.X., Li, P.F., 2015. Elastic behaviour and failure mechanism in epoxy syntactic foams: the effect of glass microballoon volume fractions. Compos Pt B-Eng. 78, 401–408. https://doi.org/10.1016/j.compositesb.2015.04.002.
Lemaitre, J., 1984. How to use damage mechanics. Nucl. Eng. Des. 80 (2), 233–245. https://doi.org/10.1016/0029-5493(84)90169-9.
Li, R., Xu, Y., Zhang, K.H., et al., 2024. A novel computational model based on molecular chain dynamics: Quantification and evaluation of interfacial interactions in polymer-based composite materials. Compos. Adv. Mater. 33, 1–12. https://doi.org/10.1177/26349833241309350.
Lin, T., Meng, W., Chen, Y.D., et al., 2023. Unloading-induced permeability recovery in rock fractures. J. Rock Mech. Geotech. Eng. 15 (12), 3148–3162. https://doi.org/10.1016/j.jrmge.2023.06.002.

Liu, G., 2019. Novel test method for the hydrostatic properties of syntactic foams. Results Mater. 1, 100010. https://doi.org/10.1016/j.rinma.2019.100010.
Liu, S.W., Lei, X., Feng, C.G., et al., 2016. Estimation of subsurface formation temperature in the Tarim Basin, northwest China: Implications for hydrocarbon generation and preservation. Int. J. Earth Sci. 105 (5), 1329–1351. https://doi.org/10.1007/s00531-015-1253-4.
Pei, L.Z., Ya, B., Huang, S.H., et al., 2025. Construction of multilevel interfacial structures and their effect on the properties of syntactic foams. Appl. Surf. Sci. 688, 162435. https://doi.org/10.1016/j.apsusc.2025.162435.
Phan, V.T., Choqueuse, D., Cognard, J.Y., et al., 2013. Experimental analysis and modelling of the long term thermo-mechanical behaviour of glass/polypropylene syntactic used on thermally insulated offshore pipeline. Prog. Org. Coating 76 (2–3), 341–350. https://doi.org/10.1016/j.porgcoat.2012.09.028.
Porfiri, M., Gupta, N., 2009. Effect of volume fraction and wall thickness on the elastic properties of hollow particle filled composites. Compos Pt B-Eng. 40 (2), 166–173. https://doi.org/10.1016/j.compositesb.2008.09.002.
Saif, T., Lin, Q., Bijeljic, B., et al., 2017. Microstructural imaging and characterization of oil shale before and after pyrolysis. Fuel 197, 562–574. https://doi.org/10.1016/j.fuel.2017.02.030.
Schumacher, G., Murray, C.M., Park, J., et al., 2024. Energy absorption behavior of elastomeric matrix composites reinforced with hollow glass microspheres. Aerospace 11 (12), 1012. https://doi.org/10.3390/aerospace11121012.
Shahapurkar, K., Garcia, C.D., Doddaman, M., et al., 2018. Compressive behavior of cenosphere/epoxy syntactic foams in arctic conditions. Compos Pt B-Eng. 135, 253–262. https://doi.org/10.1016/j.compositesb.2017.10.006.
Shi, X.J., Xie, H.P., Li, C., et al., 2025. Performance of a deep in situ pressure-preserving coring controller in a high-temperature and ultrahigh-pressure test system. J. Rock Mech. Geotech. Eng. 17 (2), 877–896. https://doi.org/10.1016/j.jrmge.2024.01.012.
Sue, R., Wang, Y.N., Cheng, Y., 2022. Research progress of syntactic foams used in solid buoyance material. J. Mater. Eng. 50 (6), 86–96. https://doi.org/10.11868/j.issn.1001-4381.2021.000566.
Sun, J.S., Liu, W., Wang, Q., et al., 2024. Challenges and development prospects of oil and gas drilling and completion in myriametric deep formation in China. Drill. Prod. Technol. 47 (2), 1–9. https://doi.org/10.3969/J.ISSN.1006-768X.2024.02.01.
Tong, Y.Q., Shi, Q.S., Liu, M.J., et al., 2021. Lightweight epoxy-based abradable seal coating with high bonding strength. J. Mater. Sci. Technol. 69, 129–137. https://doi.org/10.1016/j.jmst.2020.05.077.
Wang, J.Z., Cui, W.C., 2023. A cross-scale hygro-mechanical coupling model for hollow glass bead/resin composite materials. Int. J. Solid Struct. 264, 112104. https://doi.org/10.1016/j.ijsolstr.2023.112104.
Wei, Z., He, Z., Chen, L., et al., 2025. Properties of thermal insulation materials for deep oil and gas in situ temperature-preserved coring: A focus on interphase. J. Rock Mech. Geotech. Eng. 17 (12), 7691–7710. https://doi.org/10.1016/j.jrmge.2025.01.026.
Wei, Z.J., He, Z.Q., Yang, J.P., 2024. Analysis of core temperature variation and its influencing factors in deep rock in-situ temperature-preserved coring. Adv. Geo-Energy Res. 14 (3), 215–223. https://doi.org/10.46690/ager.2024.12.06.
Wei, Z.J., Li, C., Yu, B., et al., 2023. Study on heat transfer model theory and numerical simulation used in deep rock in-situ temperature-preserved coring. Therm. Sci. 27 (1B), 639–646. https://doi.org/10.2298/TSCI2301639W.
Wu, X., Gao, Y., Wang, Y., et al., 2021. Recent developments on epoxy-based syntactic foams for deep sea exploration. J. Mater. Sci. 56 (3), 2037–2076. https://doi.org/10.1007/s10853-020-05420-w.
Xiao, Y.M., Qiao, Y.F., He, M.C., et al., 2023. Strain rate effect of siltstone under triaxial compression and its interpretation from damage mechanics. Rock Mech. Rock Eng. 56 (12), 8643–8656. https://doi.org/10.1007/s00603-023-03528-4.
Xie, H.P., Gao, F., Ju, Y., 2015. Research and development of rock mechanics in deep ground engineering. Chin. J. Rock Mech. Eng. 34 (11), 2161–2178. https://doi.org/10.13722/j.cnki.jrme.2015.1369 (in Chinese).
Xie, H.P., Gao, M.Z., Zhang, R., et al., 2020. Study on concept and progress of in situ fidelity coring of deep rocks. Chin. J. Rock Mech. Eng. 39 (5), 865–876. https://doi.org/10.13722/j.cnki.jrme.2020.0138 (in Chinese).
Xie, H.P., Gao, M.Z., Zhang, R., et al., 2019. Study on the mechanical properties and mechanical response of coal mining at 1000m or deeper. Rock Mech. Rock Eng. 52 (5), 1475–1490. https://doi.org/10.1007/s00603-018-1509-y.
Xie, H.P., Hu, Y.Q., Gao, M.Z., et al., 2023. Research progress and application of deep in-situ condition preserved coring and testing. Int. J. Min. Sci. Technol. 33 (11), 1319–1337. https://doi.org/10.1016/j.ijmst.2023.06.007.
Xie, H.P., Ju, Y., Li, L.Y., 2005. Criteria for strength and structural failure of rocks based on energy dissipation and energy release principles. Chin. J. Rock Mech. Eng. (17), 3003–3010. https://doi.org/10.3321/j.issn:1000-6915.2005.17.001 (in Chinese).
Xie, H.P., Liu, T., Gao, M.Z., et al., 2021. Research on in-situ condition preserved coring and testing systems. Pet. Sci. 18 (6), 1840–1859. https://doi.org/10.1016/j.petsci.2021.11.003.
Xu, X.L., Karakus, M., 2018. A coupled thermo-mechanical damage model for granite. Int. J. Rock Mech. Min. Sci. 103, 195–204. https://doi.org/10.1016/j.ijrmms.2018.01.030.
Yang, J.P., Chen, L., Gu, X.B., et al., 2022. Hollow glass microspheres/silicone rubber composite materials toward materials for high performance deep in-situ temperature-preserved coring. Pet. Sci. 19 (1), 309–320. https://doi.org/10.1016/j.petsci.2021.11.012.
Zhai, G.J., Ding, Y., Ma, Z., et al., 2022. Novel triaxial experimental investigation on compressive behavior of hollow glass microspheres composites under varied temperature environments. Polym. Test. 115, 107745. https://doi.org/10.1016/j.polymertesting.2022.107745.
Zhai, G.J., Ding, Y., Wang, Y., et al., 2020. Experimental investigation of the hydrostatic compression of a hollow glass microspheres/epoxy resin under high-pressure conditions at the full ocean depth. Polym. Compos. 41 (12), 5331–5342. https://doi.org/10.1002/pc.25797.
Zhai, G.J., Wei, Z.H., Ma, Z., et al., 2023. Establishment and program development of failure criterion of hollow glass microspheres/epoxy resin composites based on tension/compression discrepancy. Eng. Fail. Anal. 149, 107270. https://doi.org/10.1016/j.engfailanal.2023.107270.
Zhang, L.H., Townsend, D., Petrinic, N., et al., 2022. The dependency of compressive response of epoxy syntactic foam on the strain rate and temperature under rigid confinement.